Dielectric constant reduction in silicon nanostructures

Han G. Yoo*
Department of Physics and Astronomy, University of Rochester, Rochester, New York 14627, USA

Philippe M. Fauchet
Department of Electrical and Computer Engineering, University of Rochester, Rochester, New York 14627, USA

(Received 30 July 2007; revised manuscript received 12 October 2007; published 28 March 2008)

We performed a systematic measurement of the dielectric function of Si nanoslabs as a function of their thickness using spectroscopic ellipsometry from 0.73 eV (1700 nm) to 4.58 eV (270 nm). The Si nanoslabs were obtained by repeatedly thinning down the top Si layer in silicon-on-insulator wafers by successive oxidation and HF etching. As predicted by the theories, both real and imaginary parts of the dielectric function are reduced as the thickness decreases. The dielectric constant of 3.3-nm-thick nanoslabs measured at 0.73 eV, below the band gap energy of bulk Si, is reduced by ~13% (from 12 to 10.4) compared to the bulk value. The measured size dependence is in qualitative but not quantitative agreement with the most applicable theory.

DOI: 10.1103/PhysRevB.77.115355 PACS number(s): 78.20.Ci, 73.22.−f, 77.22.Ch, 78.67.De

Silicon nanostructures have attracted a lot of attention because of their various potential uses from memory elements to light sources.[1–4] When designing devices that incorporate Si nanostructures, it is often important to precisely know their dielectric functions ϵ or indices of refraction n ($\epsilon=n^2$), since they determine many of their electrical and optical properties.

Several theoretical studies[5–10] have predicted a reduction in ϵ as the nanostructure size decreases. However these models propose different physical mechanisms for the reduction and arrive at different reduction factors. In one model, the reduction is due to quantum confinement effects,[5–7] which increases the band gap energy compared to the bulk value. In a more recent model, the decrease of ϵ was not attributed to the opening of the band gap, but instead to breaking of polarizable bonds on the surface—a surface effect.[8–10]

There have been numerous experimental reports on the size dependence of ϵ for various semiconductor nanostructures (e.g., PbSe nanodots in Ref. 11), but only a few have been reported for Si nanostructures.[12–16] In those few studies, the nanostructures were Si nanocrystals (nc-Si) and the value of ϵ was obtained through spectroscopic ellipsometry[12–15] and C-V measurement.[16] However, all the measurements except the one published in Ref. 12 were performed at only one particular average size, and therefore these studies could not confirm any particular theory on static dielectric constant over a range of sizes. In Ref. 12, the size of nc-Si ranged from 1.25 down to 0.6 nm, but the lowest energy at which ϵ was measured was ~3 eV for 0.6-nm-wide nc-Si.

In our work, we have systematically measured the size dependent ϵ of crystalline Si (c-Si) nanoslabs of different thicknesses from ~14 to 3.2 nm using spectroscopic ellipsometer over the spectral range of 0.73 eV (1700 nm) to 4.58 eV (270 nm). The experimentally obtained values of ϵ are then compared to the theories that have been presented so far.

The Si nanoslabs were made of small pieces of a silicon-on-insulator wafer—100 nm of (100) c-Si separated from the Si wafer by 200 nm of SiO_2 (buried oxide). The top c-Si layer thickness was first reduced to 13.8 nm (sample A), 13.1 nm (sample B), and 11.4 nm (sample C) by a wet thermal oxidation followed by removal of the top SiO_2 layer in 20:1 buffered oxide etchant (BOE). To further reduce the remaining top c-Si layer by small step size (between 1.1 and 1.9 nm), the samples repeatedly underwent dry oxidation for 5 min in a flowing argon and oxygen ambient inside a tube furnace at either 650 °C (sample A) or 600 °C (samples B and C) followed by BOE etching, producing nanosized Si slabs on the thick SiO_2 layer (Fig. 1). Spectroscopic ellipsometry was carried out in between each etching step (i.e., at different thicknesses) on the same location for each sample. Atomic force microscopy (AFM) measurements were performed on sample A when its thickness was 5.6 nm and surface profilometry was performed on sample B at 3.2 nm. To minimize the growth of native oxide, the 40-min long ellipsometry measurement was done within 10 min after the BOE etching in air at room temperature, and the samples were kept in a vacuum desiccator whenever they were not under measurement. In order to check the amount of ultrathin thermal oxide growth including possible native oxide, a bare (100) c-Si piece of size similar to each sample was placed

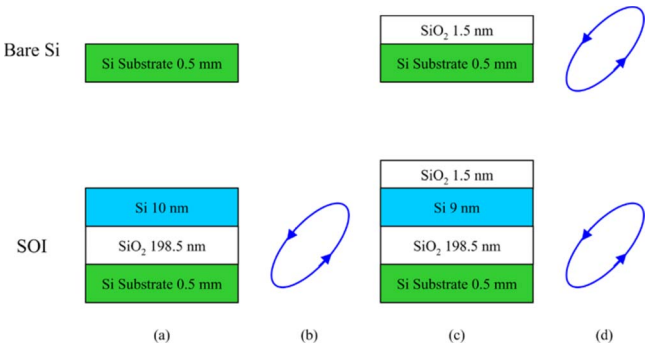

FIG. 1. (Color online) Fabrication procedure for the samples and bare Si pieces. When further thinning down the samples' top Si layer, the following sequence was repeated: (a) removal of oxidized Si by BOE etching, (b) ellipsometry measurement, (c) dry oxidation in a flowing argon and oxygen environment at either 600 or 650 °C for 5 min, and (d) ellipsometry measurement. The bare Si pieces did not undergo step (b) after BOE etching.

alongside during each oxidation and its oxide growth was measured by ellipsometry afterward.

A variable angle spectroscopic ellipsometer (J. A. Woollam vertical VASE) was used over the spectral range of 0.73–4.58 eV. The measurements were performed in steps of 0.05 eV at three different incident angles (65°, 70°, and 75°). To attain a high accuracy, each ellipsometric angle (Ψ, Δ) was acquired with a total of 50 analyzer revolutions with an adjustable retarder placed in between light source polarizer and sample, which enabled accurate measurement of Δ over the entire range of 0°–360°.[17] The incident beam was of a circular shape with a diameter of ~4 mm. The probed areas on the samples, therefore, were of an elliptical shape with the lengths of about 10, 12, and 15 mm along the lateral axis at 65°, 70°, and 75° incident angles, respectively. The measurements were taken on the same spot on each sample so as to avoid any errors due to possible SiO_2 layer thickness fluctuations.

Surface roughness and the possible presence of small pinholes were investigated over different length scales. First, three-dimensional surface profiles were acquired by a profilometer with a lateral resolution of 900 nm. For sample B with 3.2 nm thickness, the profilometer showed a few micron square pinholes and pillars over 349×262 μm^2 scanned areas with ~0.2% of surface area having the pinholes and/or pillars. The surface rms roughness was ~0.5 nm. In addition, AFM measurements with ~40 nm resolution were performed on an ~5.6-nm-thick nanoslab of sample A. The 10×10 μm^2 scan showed a very smooth surface with ~0.1% of area occupied by a handful of small pits and pillars with lateral sizes of less than 425 nm. The AFM measurement found the surface rms roughness to be ~0.4 nm, which was in good agreement with the profilometry data.

When analyzing the data, the thin Si layer was modeled by different combinations of the Kramers–Kronig consistent parametric oscillatory functions: Tauc–Lorentz (TL) and Gaussian (Gau).[17–19] These functions generated ϵ_I ($\epsilon = \epsilon_R + i\epsilon_I$) with no absorption below the band gap energy of Si (1.1 eV). The combinations of the oscillatory functions that yielded a good match with the measured data were (1) a set of one Gau and one TL and (2) a set of two TL's. The two different oscillatory function sets would slightly output different values for thickness and ϵ for the same ellipsometric data, thus providing a rough idea for the error range. The fitted variables were oscillators' parameters and layer thickness. For each sample, the model layer thickness for the buried oxide was kept fixed (e.g., 198.6 nm) for all scans as was not expected to be changed by the oxidation and etching processes. Likewise, its ϵ was fixed to the bulk value.

Since ellipsometry acquires Ψ and Δ, which are function of the product of thickness and ϵ, it is imperative that the measured thickness (and/or ϵ, if possible) be separately verified in order to confirm that the measured ϵ is reliable. As discussed above and shown in Fig. 1, along with each sample, a bare Si piece of similar size underwent the identical oxidation–etch iteration. The amount of thermal oxide growth on the bare piece was measured by the spectroscopic ellipsometry, and it ranged between 2.1 and 2.6 nm for sample A (oxidized at 650 °C) and between 1.7 and 2.4 nm for samples B and C (oxidized at 600 °C). The estimated Si reduction amount on the sample was then calculated based on the oxide growth on the bare piece, since it was expected that the same amount of oxide would grow on the sample. For all the three samples and oxidation–etch iterations, the estimated and actual reduction amounts were consistent with each other, hence confirming that the samples' Si nanoslab thickness values as obtained from the ellipsometry were reliable.

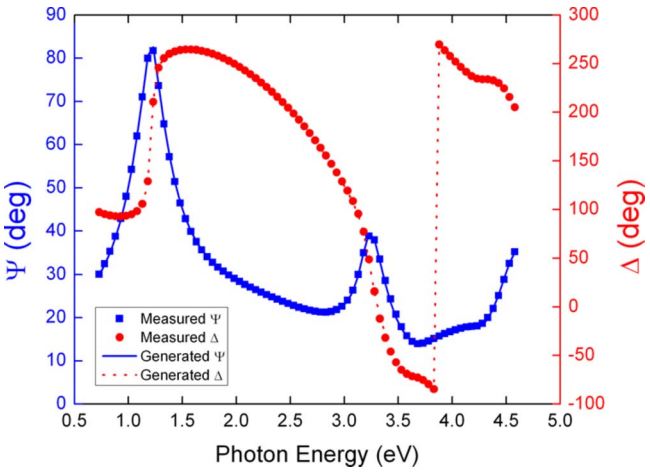

FIG. 2. (Color online) Ellipsometric angles Ψ and Δ of both measured and fit data sets at the incident angle of 65° for a 3.5-nm-thick Si layer of sample C. The filled squares and circles represent the measured Ψ and Δ, respectively. The solid and dotted curves represent the fitted Ψ and Δ, respectively, generated by fitting the measured data with two TL oscillators. The fit matches the measured data very well over the entire spectrum.

Since ellipsometry is a model-based technique, the resulting best-fit model must be evaluated for fit error and physical meaningfulness. In terms of fit statistics, a fitted model was counted in the final analysis if the mean square error (MSE) was approximately ten or less, the error bars for all fit parameters were less than 10% of the fit values, and all parameters were uncorrelated with one another. The energy peaks of the fitted Si layer's ϵ_I were also checked to verify that they were between 3 and 5 eV—close to the energy peaks for bulk 3.4 and 4.2 eV—as quantum confinement or surface polarization effect was not expected to change the peak position outside this range. Figure 2 illustrates the quality of the fits. Since the fit matches the measured data very well over the entire spectrum, the ϵ and thickness values deduced from the fit accurately represent the measurement.

The possible influence of surface roughness (SR) in the ellipsometric data analysis was considered by including an SR layer. The dielectric function of the SR layer was modeled using an effective medium approximation (EMA) with 50% of void and 50% of the ultrathin Si layer.[17] The model for the sample then consisted of *c*-Si substrate, SiO_2 layer, the ultrathin Si layer, and the SR layer, all with perfectly uniform thicknesses. After fitting the model against measured data, the best fit yielded an SR layer's thickness of between 0 and 0.5 nm.

Since Si is transparent in the spectral range below its band gap energy of 1.1 eV, the ϵ measured at 0.73 eV (the lowest

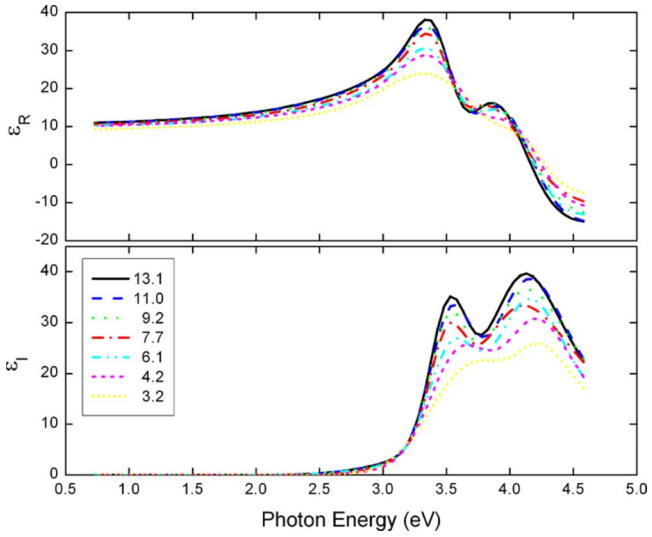

FIG. 3. (Color online) Measured ϵ_R and ϵ_I over the entire spectrum vs layer thickness from 13.1 to 3.2 nm for sample B, incorporating no SR layer in the fit. The oscillatory functions used in the fit are TL and Gau.

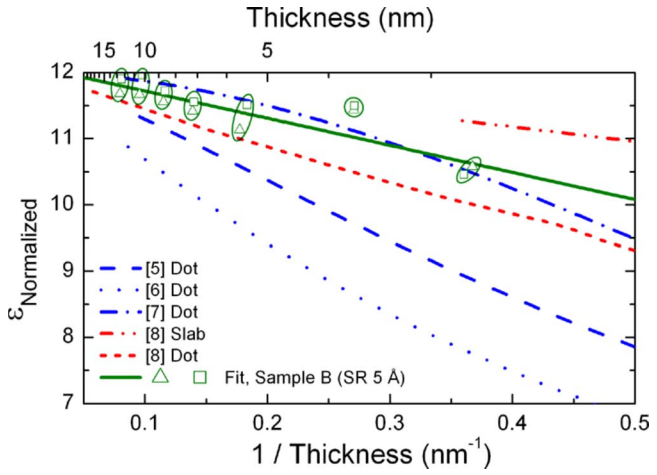

FIG. 4. (Color online) Comparison of theories and measurement. Plots of measured and theoretical ϵ are shown as a function of the inverse thickness (or diameter for nanodots). For clarity, the data from only sample B are shown for the measurement, but the solid line represents a linear fit to all the measured $\epsilon_{normalized}$ for all three samples. Two different sets of oscillatory functions were used: a set of TL and Gau (triangles) and a set of two TL oscillators (squares). The fit incorporated an SR layer of 5 Å. Each ellipsometric data were evaluated with the two sets and the two resulting fits are grouped together. The blue dotted curves represent the theoretical calculations based on quantum confinement effect for a nanodot; the red curves correspond to the surface polarization effect calculations for a nanoslab and nanodot. All ϵ are linearly scaled such that their respective bulk values are 12.

spectral energy available from the ellipsometer) was selected to be compared to the static ϵ predicted by the theories. At 0.73 eV, ϵ_R is not affected by a possible broadening of the two electronic transition resonances near 3.4 and 4.2 eV. Figure 3 shows the measured ϵ_R and ϵ_I for sample B (without an SR layer in the fit) over the entire spectrum at its various thicknesses from 13.1 down to 3.2 nm. It shows that the absolute values of ϵ_R and ϵ_I decrease overall as the thickness decreases.

The known value for ϵ_{bulk} at 0.73 eV is 12.[20] Our ellipsometric measurements performed with a layer thickness of ~13.5 nm yielded a value of ~11.5, which was taken as the measured ϵ_{bulk}. The theoretical models predicting the behavior of ϵ as a function of size used different values for ϵ_{bulk} (10.4,[5] 10.6,[8] 11.3,[7] or 11.4[6]). To compare the theoretical predictions and our measurements, we decided to normalize both to $\epsilon_{bulk\ normalized}=12$. The rescaling of the measurements or theoretical predictions was performed using the following expression:

$$\epsilon_{normalized} = 1 + \frac{\epsilon_{bulk\ normalized} - 1}{\epsilon_{bulk} - 1}(\epsilon_{un\text{-}normalized} - 1), \quad (1)$$

where $\epsilon_{un\text{-}normalized}$ is the measured or calculated value for a given size and ϵ_{bulk} is the value measured for 13.5-nm-thick films or the bulk value used in the calculations.

Between the two competing theories, the quantum confinement effect theories for nanodots[5–7] are based on the generalized Penn model (GPM), expressed as

$$\epsilon(R) = 1 + \frac{\epsilon_{bulk} - 1}{1 + (\alpha/R)^l}, \quad (2)$$

where R is the radius of the nanodots. On the other hand, the surface polarization effect theory[8,9] considers a nanostructure to have two regions—surface and core—with different dielectric values. The surface region of depth $d_{surface}$ (or equivalently volume $V_{surface}$) has the dielectric value of $\epsilon_{surface}$, whereas the rest of the region (core) that of ϵ_{bulk}. The dielectric value of an isolated nanoslab with two surface regions (one on each surface) as a whole then becomes

$$\epsilon(R) = \epsilon_{bulk} - (\epsilon_{bulk} - \epsilon_{surface})\frac{d_{surface}}{R} = \epsilon_{bulk} - \frac{s}{R}, \quad (3)$$

where $2R$ is defined to be the total slab thickness and $s = (\epsilon_{bulk} - \epsilon_{surface})d_{surface}$. Noteworthy is the similarity between the surface polarization effect expression [Eq. (3)] and the first-order approximation of the GPM,

$$\epsilon(R) \simeq \epsilon_{bulk} - (\epsilon_{bulk} - 1)\left(\frac{\alpha}{R}\right)^l, \quad (4)$$

which is formulated by expanding the GPM as a power series given $(\alpha/R)^l < 1$ for all R of interest. From Eq. (4), the surface polarization effect expression can be obtained by setting $l=1$ and replacing $\epsilon_{bulk}-1$ with $\epsilon_{bulk}-\epsilon_{surface}$. It is to be noted that the two competing theories both exhibit $(1/R)^l$ dependence.

On Fig. 4, the measured $\epsilon_{normalized}$ are plotted along with theoretically calculated $\epsilon_{normalized}$ as a function of the reciprocal of the nanoslab thickness or nanodot diameter. For clarity, the measured values for only sample B are shown, but the solid straight line represents a linear fit to all the measured $\epsilon_{normalized}$ for all three samples [A, B, and C] combined.

Since each measured ellipsometric data were fitted with two different sets of oscillatory functions, there are for each data two slightly different fitted values for thickness and $\epsilon_{normalized}$. The triangles represent the fit with TL and Gau oscillators and the squares designate the fit with two TL oscillators. These two fit results for the same ellipsometric data are grouped together, giving a general clue to the data's error range. Given the surface roughness obtained from the AFM and surface profilometry, the fits were evaluated with a 0.5 nm SR layer in the fit. For all three samples' data, the value of ϵ is only weakly dependent on the choice of the parametric oscillatory functions mentioned above. The trend is that of a clear reduction when the thickness decreases below 10 nm. Since the measurement was for nanoslab, the theoretical prediction on slab in Ref. 8 should provide a better fit to the measured ϵ.

Experimental observation of the surface polarization effect is highly susceptible to surface conditions, one of which is surface roughness. It is essential to distinguish the ϵ reduction due to the purported surface polarization effects as proposed in Ref. 8 from the decrease simply due to surface roughness. As mentioned above, the possible influence of surface roughness was evaluated by including an SR layer above the Si slab, which was modeled by EMA with 50% of ϵ_{void} and the ϵ of the Si slab. As revealed by the profilometry and AFM measurements, the upper bound for the SR layer thickness can be estimated to be ~0.5 nm. To get a better idea on how the SR layer thickness affects the ϵ and thickness, the ellipsometric data were reevaluated with 0, 1, 1.5, and 2 nm of SR layer for comparison. As the SR layer thickness increases, the nanoslab thickness becomes smaller and ϵ of the slab becomes larger. For SR layer thicknesses beyond 0.5 nm, the MSE of the fit rises; beyond 1 nm, ϵ becomes higher than the bulk value to compensate for the arbitrarily decreased nanoslab thickness. Hence, the best fit is obtained for a 0.5-nm-thick SR layer. The different trends with varying SR layer thicknesses are shown in Fig. 5 along with the prediction based on surface polarization effect for nanoslab.[8] If a 0.8-nm-thick SR layer was incorporated in the fitting, the resulting ϵ trend would match that of the theoretical plot. As discussed above, the quality of the fit degrades if the SR layer thickness is greater than 0.5 nm; therefore, the fit with a 0.5-nm-thick SR layer is compared to the theoretical prediction.

Note that a potential effect of the surface roughness in between the Si slab and the buried oxide layer underneath was not taken into account in the ellipsometry analysis. Given the trend shown in Fig. 5 with different SR layer thicknesses, the inclusion of another SR layer (with ϵ of SiO_2, not ϵ_{void}) in between the slab and the oxide layer would produce a plot line that matches closer to the theoretical prediction. In addition, the Si slab modeled in Ref. 8 is an isolated structure with both surfaces terminated by hydrogen atoms. It is conceivable that the surface layer adjacent to the SiO_2 layer would exhibit a different ϵ than the theoretical model above.

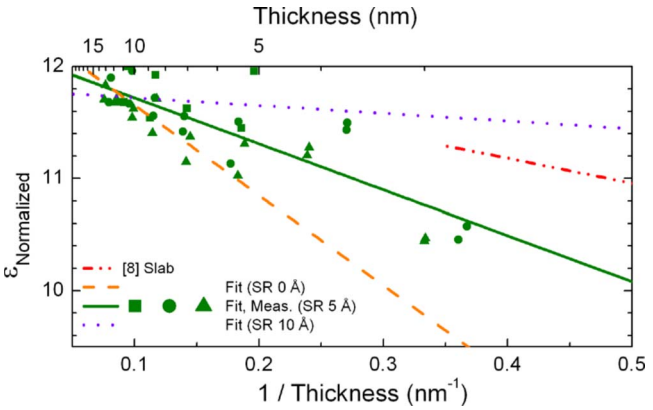

FIG. 5. (Color online) Comparison of surface polarization effect theory and measurement evaluated with an SR layer. The red dash-dot-dot curve corresponds to the surface polarization effect calculation for a nanoslab shown in Ref. 8. The plot points for samples A, B, and C are marked with squares, circles, and triangles, respectively. The filled data marks represent the measured ϵ values evaluated with 5 Å of SR layer for all three samples using the two different oscillator sets, and the solid line is a linear fit to the data. The linear fit lines to the data evaluated with 0 Å (dash) and 10 Å (dot) of SR layer are also shown.

In conclusion, the dielectric function of ultrathin Si nanoslabs has been measured by variable angle spectroscopic ellipsometer as their thicknesses decreased from 13.8 to 3.3 nm. The dielectric value at 0.73 eV is reduced by ~13% (from 12 to 10.4) compared to the bulk value. The data are in qualitative but not quantitative agreement with a theory based on the surface polarization effect and obtained for isolated Si slabs.

The authors thank the Optical Manufacturing Group at the University of Rochester's Laboratory for Laser Energetics for use of the ellipsometer and profiler. H.G.Y. thanks R. Krishnan and T. Tiwald for assistance with ellipsometry and fruitful discussion. This study was supported by the (U.S.) Air Force Office of Scientific Research's MURI Program (FA9550-06-1-0470) and (U.S.) Army Research Office (DAAD19-03-1-0267).

*hgyoo@pas.rochester.edu

[1] S. Tiwari, F. Rana, H. Hanafi, A. Hartstein, E. F. Crabbe, and K. Chan, Appl. Phys. Lett. **68**, 1377 (1996).
[2] A. D. Yoffe, Adv. Phys. **50**, 1 (2001).
[3] K. D. Hirschman, L. Tsybeskov, S. P. Duttagupta, and P. M. Fauchet, Nature (London) **384**, 338 (1996).
[4] L. Pavesi, L. Dal Negro, C. Mazzoleni, G. Franzo, and F. Priolo, Nature (London) **408**, 440 (2000).
[5] L. W. Wang and A. Zunger, Phys. Rev. Lett. **73**, 1039 (1994).
[6] M. Lannoo, C. Delerue, and G. Allan, Phys. Rev. Lett. **74**, 3415

(1995).
[7] R. Tsu, D. Babic, and L. Ioriatti, J. Appl. Phys. **82**, 1327 (1997).
[8] C. Delerue, M. Lannoo, and G. Allan, Phys. Rev. B **68**, 115411 (2003).
[9] C. Delerue and G. Allan, Appl. Phys. Lett. **88**, 173117 (2006); **89**, 129903 (2006).
[10] F. Trani, D. Ninno, and G. Iadonisi, Phys. Rev. B **75**, 033312 (2007).
[11] Z. Hens, D. Vanmaekelbergh, E. S. Kooij, H. Wormeester, G. Allan, and C. Delerue, Phys. Rev. Lett. **92**, 026808 (2004).
[12] H. V. Nguyen, Y. Lu, S. Kim, M. Wakagi, and R. W. Collins, Phys. Rev. Lett. **74**, 3880 (1995).
[13] D. Amans, S. Callard, A. Gagnaire, J. Joseph, G. Ledoux, and F. Huisken, J. Appl. Phys. **93**, 4173 (2003).
[14] M. Losurdo, M. Giangregorio, P. Capezzuto, G. Bruno, M. Cerqueira, E. Alves, and M. Stepikhova, Appl. Phys. Lett. **82**, 2993 (2003).
[15] K. Lee, T. Kang, H. Lee, S. Hong, S. Choi, T. Seong, K. Kim, and D. Moon, Thin Solid Films **476**, 196 (2005).
[16] C. Ng, T. Chen, L. Ding, Y. Liu, M. Tse, S. Fung, and Z. Dong, Appl. Phys. Lett. **88**, 063103 (2006).
[17] H. G. Tompkins and E. A. Irene, *Handbook of Ellipsometry* (Springer, Heidelberg, 2005).
[18] G. E. Jellison and F. A. Modine, Appl. Phys. Lett. **69**, 371 (1996).
[19] A. S. Ferlauto, G. M. Ferreira, J. M. Pearce, C. R. Wronski, R. W. Collins, X. Deng, and G. Ganguly, J. Appl. Phys. **92**, 2424 (2002).
[20] E. D. Palik, *Handbook of Optical Constants of Solids* (Academic, San Diego, 1998).